ANALYSIS OF DIFFERENT STRATEGIES FOR INCORPORATING SPATIAL INFORMATION IN THE DESIGN OF ENDMEMBER EXTRACTION ALGORITHMS FROM HYPERSPECTRAL DATA

Gabriel Martín, Antonio Plaza

Department of Computer Science,
University of Extremadura,
E-10071 Cáceres, Spain.

Maciel Zortea

Department of Mathematics and Statistics,
University of Tromso,
N-9037, Tromso, Norway.

ABSTRACT

Over the last decade, several algorithms have been developed for automatic or semi-automatic extraction of spectral endmembers from hyperspectral image data. In this paper, we present a thorough analytical comparison of endmember extraction methods which include spatial information in the search of spectral endmembers versus a few algorithms which are exclusively based on spectral information. Our quantitative and comparative assessment of algorithm accuracy and computational performance, conducted using both synthetic and real hyperspectral data, provides interesting findings about the potential benefits that can be obtained after incorporating spatial information into the design of endmember extraction algorithms.

Index Terms— Spatial-spectral endmember extraction, spectral unmixing, fractional abudance estimation.

1. INTRODUCTION

Endmember extraction is the process of selecting a collection of pure signature spectra of the materials present in a remotely sensed hyperspectral scene [1]. These pure signatures are then used to decompose the scene into abundance fractions by means of a spectral unmixing algorithm. Over the last decade, several algorithms have been developed for automatic or semi-automatic extraction of spectral endmembers from the hyperspectral image data. Classic techniques include the pixel purity index (PPI) [2], the N-FINDR algorithm [3], the vertex component algorithm (VCA) [4], an iterative error analysis (IEA) algorithm [5], the optical real-time adaptive spectral identification system (ORASIS) [6], the convex cone analysis (CCA) algorithm [7], and an orthogonal subspace projection (OSP) technique [8]. Other advanced techniques for endmember extraction have been recently proposed, including ICE [9], a statistical approach, a minimum volume constrained nonnegative matrix factorization approach [10], a simplex growing algorithm (SGA) [11], a technique based on independent component analysis (ICA) [12], a support vector algorithm for detecting endmembers [13], or a technique based on the concept of sparsity [14], among others [1]. Most of these techniques have been focused on analyzing the hyperspectral data without incorporating information on the spatially adjacent data. As a result, the search is conducted by treating the data as a collection of spectral measurements with no spatial arrangement. However, one of the distinguishing properties of hyperspectral data is the multivariate information coupled with a two-dimensional (pictorial) representation amenable to image interpretation. Subsequently, most endmember extraction algorithms listed above could benefit from an integrated framework in which both the spatial and the spectral information are considered. However, only a few attempts exist in the literature aimed at including the spatial information in the process of extracting spectral endmembers, including the automatic morphological endmember extraction (AMEE) [15], the spatial spectral endmember extraction (SSEE) [16], and a recently developed spatial preprocessing (SPP) approach [17].

In this paper, we present a thorough analytical comparison of methods including spatial information (AMEE, SSEE, SPP) and a few selected algorithms which are exclusively based on spectral information[1]. Our experimental assessment of endmember extraction accuracy has been conducted using both synthetic and real hyperspectral data. The synthetic scenes were artificially generated using fractals to simulate naturally-inspired spatial patterns, combined with spectral signatures obtained from different spectral libraries. The real hyperspectral scene was collected by the Jet Propulsion Laboratory's Airborne Visible Infra-Red Imaging Spectrometer (AVIRIS) over the Cuprite region in Nevada.

The remainder of the paper is organized as follows. Section 2 describes the AMEE, SSEE and SPP methods for joint spatial-spectral endmember extraction. Section 3 describes the synthetic and real hyperspectral data sets used in this study. Section 4 presents a detailed algorithm comparison in terms of endmember extraction accuracy and computational performance. Section 5 concludes with some remarks.

[1] All the methods compared in this work have been implemented using the Orfeo toolbox distributed by CNES, see http://www.orfeo-toolbox.org

2. METHODS

This section describes the spatial-spectral endmember extraction methods considered in this work: AMEE, SSEE and SPP. The latter can be combined with spectral-based methods.

2.1. AMEE

The AMEE algorithm runs on the full data cube with no dimensional reduction, and begins by searching spatial neighborhoods around each pixel in the image for the most spectrally pure and mostly highly mixed pixel. This task is performed by using extended mathematical morphology operators of dilation and erosion, respectively. Each spectrally pure pixel is assigned an "eccentricity" value, which is calculated as the spectral angle distance between the most spectrally pure and mostly highly mixed pixel for the given spatial neighborhood. This process is repeated iteratively for larger spatial neighborhoods up to a maximum size that is pre-determined. At each iteration the "eccentricity" values of the selected pixels are updated. The final endmember set is obtained by applying a threshold to the resulting greyscale "eccentricity" image. The final endmembers are extracted after a region growing process.

2.2. SSEE

The SSEE algorithm comprises four steps. First, it divides the scene in sub regions and applies singular value decomposition for obtaining a set of eigenvectors that explain most of the spectral variability of each particular spatial subset. Then, it projects the entire image data onto the compiled eigenvector set to determine a set of candidate endmember pixels representative of all image. In a third step, the algorithm analyzes the spatial and spectral characteristics of the candidate endmember set to average spectrally similar endmember candidates that are spatially related. Finally, the endmember set derived in the previous step is reordered based on spectral angle, thus listing endmember candidates in order of spectral similarity (from highest to lowest similarity).

2.3. SPP

The SPP method can be easily used in combination with available imaging spectral-based endmember extraction algorithms such as those methods in [2, 3, 4, 8, 11]. This approach estimates, for each pixel vector, a scalar, spatial-derived factor which relates to the spectral similarity of pixels lying within a certain spatial neighborhood. This scalar value is then used to weight the importance of the spectral information associated to each pixel in terms of its spatial context. Two key aspects of the preprocessing approach are: 1) no modification of existing endmember extraction methods is necessary to apply the proposed approach, and 2) the method directs the search for spectral endmembers to spatially homogeneous areas.

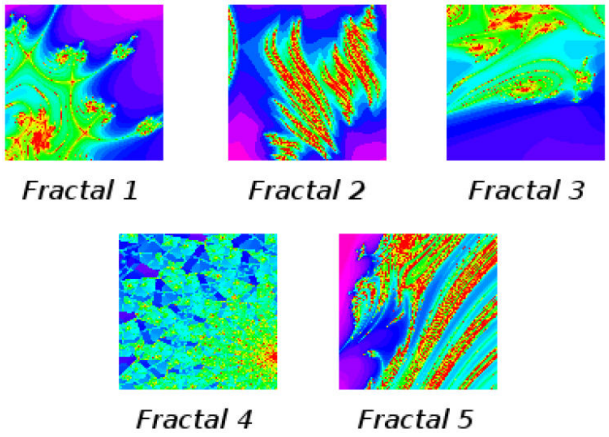

Fig. 1. Synthetic images used in experiments, where spatial patterns where generated using fractals.

3. HYPERSPECTRAL DATA SETS

3.1. Synthetic hyperspectral data

A database of five 100×100-pixel synthetic hyperspectral scenes (see Fig. 1) has been created using fractals to generate distinct spatial patterns, which are then used to simulate linear mixtures of nine reflectance signatures randomly selected from a spectral library compiled by the U.S. Geological Survey (USGS)[2]. Zero-mean Gaussian noise was added to the scenes in different signal to noise ratios (SNRs) –from 30:1 to 110:1– to simulate contributions from ambient and instrumental sources, following the procedure described in [8].

3.2. Real hyperspectral data

A well-known hyperspectral data set has been selected for the purpose of illustrating the spectral unmixing algorithm described in this work. The data set was collected by the AVIRIS sensor over the Cuprite mining district in Nevada, and is available online in both radiance and reflectance units[3]. In our experiments, we use reflectance data in order to relate our results to the reference USGS spectral library. The scene selected for experiments comprises 350×350 pixels (20-meter spatial resolution) and 188 spectral bands after removing water absorption and low SNR bands.

4. EXPERIMENTAL RESULTS

4.1. Experiments with synthetic data

In order to ensure the fairest possible comparison, we have individually optimized the parameters of each method to achieve the best possible result, and report only the best result obtained for each algorithm with each scene.

[2] http://speclab.cr.usgs.gov/spectral-lib.htm
[3] http://aviris.jpl.nasa.gov/html/aviris.freedata.html

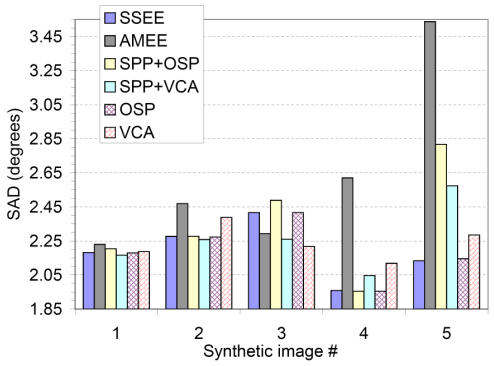

Fig. 2. Comparison of different endmember extraction algorithms in terms of average SAD score, using the five synthetic scenes in Fig. 1 with SNR of 30:1.

Fig. 2 displays the average spectral angle distance (SAD) between the endmembers extracted by different methods and reference USGS spectral signatures for the five synthetic scenes in Fig. 1 with simulated noise at SNR of 30:1. Lower SAD indicates higher spectral similarity. As shown by Fig. 2, the use of spatial information only seemed to help in certain cases, such as in the synthetic scenes 4 and 5 in which SSEE provided the most spectrally similar endmembers with regards to USGS signatures. However, AMEE provided the worst results in four out of five synthetic scenes. Further, the SPP module did not always improve the results provided by the corresponding spectral-based algorithm. These results should be analyzed in future work in order to fully substantiate whether spatial information can help identifying better endmembers (in terms of highest spectral quality).

4.2. Experiments with real data

In order to analyze the quality of fractional abundance estimations in real data, our assumption is that a set of high-quality endmembers (and the abundance fractions estimated using those endmembers and the fully constrained linear mixture model [18]) may allow reconstructing the original hyperspectral scene with highest precision than a set of low-quality endmembers. In other words, the reconstruction error, which can be seen as an indirect assessment of the the accuracy of both the endmember extraction and the linear spectral unmixing stages. Fig. 3 graphically represents the per-pixel root mean square error (RMSE) obtained after reconstructing the AVIRIS Cuprite scene using $p = 14$ endmembers extracted by different methods. It can be seen that the methods using spatial preprocessing (SPP+OSP, SPP+N-FINDR, SPP+VCA) improve their respective spectral-based versions, while both AMEE and SSEE also provide lower reconstruction errors than OSP, N-FINDR and VCA. For illustrative purposes, the error distribution patterns in 3 are shown in Fig. 4 using a different format. For each considered endmember extraction algorithm, a different plot is used to indicate how the reconstruction RMSE grows for different error bounds (percentiles) of the total measured error.

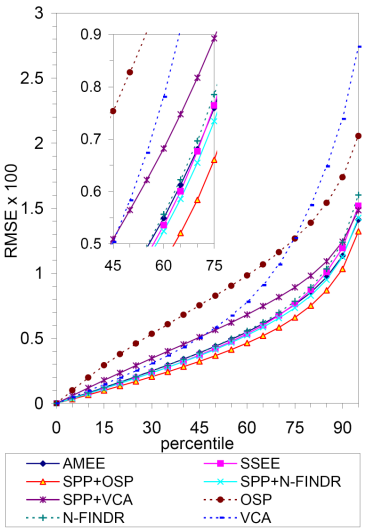

Fig. 4. Increase of reconstruction RMSE for different error bounds (percentiles) of the total measured error for the different endmember extraction algorithms.

To conclude this section, we provide an estimate of the processing time for the different endmember extraction algorithms tested in this work (unmixing time not included). The computing environment was an Intel Dual Core T2400 processor with 1.66 GHz, main memory of 2 GB and 2 MB of cache. The slowest algorithm was SSEE (24 minutes to process the AVIRIS Cuprite scene). The fastest algorithm was AMEE (73 seconds). N-FINDR (5 minutes) and OSP (11 minutes) provided intermediate processing times. The SPP module only employed 30 seconds. The processing times are quite dependent of input parameters, such as the window size in AMEE and SPP-based methods.

5. CONCLUSIONS

We have analyzed the impact of including spatial information when searching for spectral endmembers in hyperspectral scenes. The results produced by the algorithms tested in this study have been analyzed and discussed in terms of endmember signature purity, using five synthetic scenes with spatial patterns generated using fractals, and also in terms of reconstruction error, using a hyperspectral scene collected by NASA's AVIRIS instrument over the Cuprite mining district in Nevada. Our experimental results indicate that spatial information can reduce the errors in the reconstruction of the original scene using a fully constrained linear mixture model. However, it is not clear from our experiments if spatial information can provide better endmembers (in terms of higher

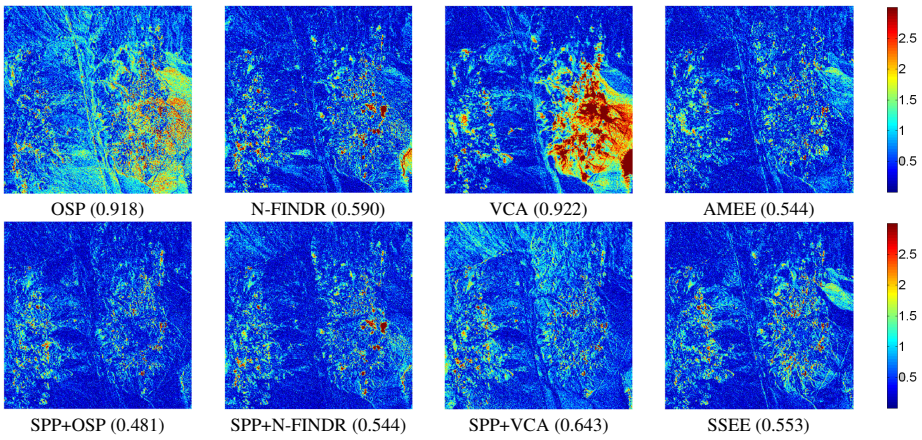

Fig. 3. RMSE reconstruction errors (multiplied by 100) for various endmember extraction algorithms (AVIRIS Cuprite).

spectral quality). Further experiments shall be conducted to fully substantiate the above remarks in different application scenarios.

6. REFERENCES

[1] A. Plaza, P. Martinez, R. Perez, and J. Plaza, "A quantitative and comparative analysis of endmember extraction algorithms from hyperspectral data," *IEEE Trans. Geosci. Remote Sens.*, vol. 42, no. 3, pp. 650-663, 2004.

[2] J. W. Boardman, F. A. Kruse, and R. O. Green, "Mapping target signatures via partial unmixing of AVIRIS data," *Proc. JPL Airborne Earth Sci. Workshop*, pp. 23-26, 1995.

[3] M. E. Winter, "N-FINDR: an algorithm for fast autonomous spectral endmember determination in hyperspectral data," *Proc. SPIE Image Spectrometry*, vol. 3753, pp. 266-277, 2003.

[4] J. Nascimento and J. Dias, "Vertex component analysis: a fast algorithm to unmix hyperspectral data," *IEEE Trans. Geosci. Remote Sens.*, vol. 43, pp. 898-910, 2005.

[5] R. A. Neville, K. Staenz, T. Szeredi, J. Lefebvre, and P. Hauff, "Automatic endmember extraction from hyperspectral data for mineral exploration," *Proc. 21st Canadian Symp. Remote Sens.*, pp. 21-24, 1999.

[6] J. H. Bowles, P. J. Palmadesso, J. A. Antoniades, M. M. Baumback, and L. J. Rickard, "Use of filter vectors in hyperspectral data analysis," *Proc. SPIE Infrared Spaceborne Remote Sensing III*, vol. 2553, pp. 148-157, 1995.

[7] A. Ifarraguerri and C.-I. Chang, "Multispectral and hyperspectral image analysis with convex cones," *IEEE Trans. Geosci. Remote Sens.*, vol. 37, no. 2, pp. 756-770, 1999.

[8] J. C. Harsanyi and C.-I. Chang, "Hyperspectral image classification and dimensionality reduction: An orthogonal subspace projection," *IEEE Trans. Geosci. Remote Sens.*, vol. 32, no. 4, pp. 779-785.

[9] M. Berman et al., "ICE: a statistical approach to identifying endmembers in hyperspectral images," *IEEE Trans. Geosci. Remote Sens.*, vol. 42, no. 10, pp. 2085-2095, 2004.

[10] L. Miao and H. Qi, "Endmember extraction from highly mixed data using minimum volume constrained nonnegative matrix factorization," *IEEE Trans. Geosci. Remote Sens.*, vol. 45, no. 3, pp. 765-777, 2007.

[11] C.-I. Chang, C.-C. Wu, W. Liu, and Y.-C. Ouyang, "A new growing method for simplex-based endmember extraction algorithm," *IEEE Trans. Geosci. Remote Sens.*, vol. 44, no. 10, pp. 2804-2819, 2006.

[12] J. Wang and C.-I. Chang, "Applications of independent component analysis in endmember extraction and abundance quantification for hyperspectral imagery," *IEEE Trans. Geosci. Remote Sens.*, vol. 44, no. 9, pp. 2601-2616, 2006.

[13] A. Banerjee, P. Burlina, and J. Broadwater, "A machine learning approach for finding hyperspectral endmembers," *Proc. IEEE Intl. Geosci. Remote Sens. Symp. (IGARSS)*, pp. 3817-3820, Barcelona, Spain, 2007.

[14] A. Zare and P. Gader, "Hyperspectral band selection and endmember detection using sparsity promoting priors," *IEEE Geosci. Remote Sens. Lett.*, vol. 5, no. 2, pp. 256-260, 2008.

[15] A. Plaza, P. Martinez, R. Perez, and J. Plaza, "Spatial/spectral endmember extraction by multidimensional morphological operations," *IEEE Trans. Geosci. Remote Sens.*, vol. 40, no. 9, pp. 2025-2041, 2002.

[16] D. M. Rogge, B. Rivard, J. Zhang, A. Sanchez, J. Harris, and J. Feng, "Integration of spatial-spectral information for the improved extraction of endmembers," *Remote Sens. Environ.*, vol. 110, no. 3, pp. 287-303, 2007.

[17] M. Zortea and A. Plaza, "Spatial preprocessing for endmember extraction," *IEEE Trans. Geosci. Remote Sens.*, accepted for publication, 2009.

[18] C.-I Chang, *Hyperspectral imaging: Techniques for Spectral Detection and Classification*, Kluwer: New York, 2003.